FORMING SIMULATIONS OF MULTI-LAYERED WOVEN PREFORMS ASSEMBLED WITH STITCH YARNS

S. Chen, A. Endruweit, L. T. Harper*, N. A. Warrior

Polymer Composites Group, Division of Materials, Mechanics & Structures, Faculty of Engineering, The University of Nottingham, UK, NG7 2RD
**lee.harper@nottingham.ac.uk*

Abstract
A model has been developed to predict the draping behaviour of thick fibre preforms with localised stitching, to analyse the forming behaviour of 3D components. Explicit finite element simulations have been performed for a hemisphere geometry to understand the influence of adding local stitch-bonds, which are used to join multiple 2D plies together for easier in-mould assembly. Stitch-bonded fibrous reinforcements are modelled as multi-layered 2D continua with additional 1D through-thickness fixations. Results demonstrate that stitch-bonds influence the global shear angle distribution in each ply of the component rather than having just a localised effect, with the most significant effects observed when placing stitches between plies of different orientations.

Keywords: Fabric drape, Finite Element Analysis, stitching, multi-ply preform

1. Introduction

Production of composite components for mid- to high-volume applications is frequently based on preforming of fibrous reinforcement structures to the geometry of the component, followed by impregnation with a thermoset resin. The challenge in introducing advanced preforming technologies is characterising the forming behaviour of 2D reinforcements in order to produce repeatable 3D components.

Previous research on reinforcement forming has mainly addressed the simulation of components consisting of a single fabric ply [1, 2], or preforms of multiple plies with identical orientation [3, 4], where inter-ply friction is not as significant as in heterogeneous multi-ply preforms [5, 6]. Little work has been reported on forming of complex stacking patterns or multi-ply preforms containing localised stitch-bonds.

One approach for simulation of multi-ply forming is to use multi-layered membrane finite elements, where one layer of membranes represents multiple fabric layers, for more efficient simulation [6]. However, this method ignores relative sliding between plies, which is one of the main forming modes for multi-ply systems. In order to account for the necessary sliding, each ply needs to be modelled independently as a separate element layer. Cheruet et al. [7] modelled forming of a Z-shaped reinforcement consisting of 10 pre-impregnated plies. Predicted relative sliding agreed well with experimental data, and it was concluded that the through-thickness stress depends on the geometry of the tool, being near-zero in most locations except in the vicinity of sharp radii. Harrison et al. [8] conducted forming simulations for two cross plies (0°/90° UD) of thermoplastic prepreg, assuming a biaxial

constitutive relationship. The viscous nature of the matrix material ensured that the main in-plane deformation mode was trellising (shear), similar to a woven material. However, when the fibres are dry, the deformation mechanism changes and intra-ply sliding becomes more important, particularly for multi-ply forming of NCF [9]. Experimental results show that NCFs experience high levels of slip within each layer of the bidirectional material, as the stitches provide less restraint than interweaving of warp- and weft-yarns. This phenomenon was captured in simulations by using bar elements to represent the stitch between UD plies modelled as shell elements. Good agreement was shown between numerical simulations and experimental results for forming of a hemisphere, but sliding was limited to just the fibre direction, which may be an oversimplification for more complex geometries.

Investigations into the influence of stitches have been generally limited to studying intra-ply stitches in NCFs [9] or single woven plies [3], to understand how they can be used to control local yarn angles. Molnar et al. [4] investigated the influence of stitching via experimental studies, which indicated that local stitch-bonds affect shear deformation, and the stitch pattern influences the quality of the formed geometry. It was concluded that it is possible to transfer shear forces into un-sheared regions during forming. Through-thickness stitching in multi-ply preforms has been successfully simulated in explicit finite element analyses using spot weld constraints [3, 10]. Whilst only multi-ply stacks with identical ply orientations were studied, this work showed that it is possible to use stitches to redistribute strains within the fabric to avoid wrinkling. Duhovic et al. [3] looked at the force-displacement relationship for the stitch in detail, incorporating a strain offset to account for slack during tensile loading. Consequently, it was found that the stitch did not restrict the material's shear behaviour when the slack was set to 19 % strain to match physical experiments. The influence of local stitch-bonds on preforming of helicopter side frames was investigated by Bel et al. [11]. Beam spring elements were used to model the stitches in explicit FE studies.

This paper presents details of a finite element model that has been developed to study the effect of introducing local stitch-bonds in multi-ply preforms, particularly those that consist of multiple ply orientations. Results are presented from a study using a simple hemisphere tool to demonstrate the capability of simulating the forming behaviour of a multi-ply stack in a single operation.

2. Material model for non-orthogonal biaxial materials

2.1. Homogenisation and hypo-elastic material model

The proposed material model captures the dominant factors in composite draping, including in-plane shear, fibre elongation and inter-tow/intra-ply slipping. A macro-scale homogenisation scheme has been adopted to avoid modelling discrete fibres/tows. The effects of parameters associated with the fibre architecture (yarn spacing, cross-sectional shape, crimp etc.) are captured in the in-plane shear behaviour, which is defined by a non-linear stress-strain curve with a progressive hardening step. A hypo-elastic model [5, 12] has been adopted to capture both material and geometric non-linearities due to large displacements and large shear deformations of the yarns [5, 12, 13]. The material is considered to be elastic, which seems appropriate in view of the reversible deformation phenomena and processes for technical textiles. However, there is the potential to develop the model to account for non-linear visco-elasticity/visco-plasticity whilst maintaining a relatively simple formulation.

A VFABRIC subroutine has been developed for Abaqus/Explicit to define the mechanical constitutive relations of woven fabrics. The VFABRIC routine is valid for materials that exhibit two structural directions, which may not remain orthogonal following deformation. This reduces the number of tensor operations and results in a more efficient model compared with a more commonly used VUMAT routine.

2.2. Implementation in user-defined subroutine

The non-orthogonal material model has been implemented in a VFABRIC material routine for Abaqus/Explicit, summarised in Figure 1.

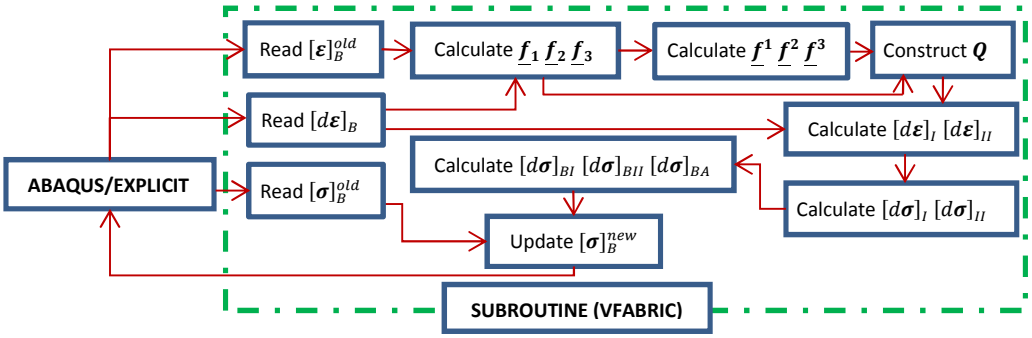

Figure 1. Flow chart of user-defined fabric material for preforming in VFABRIC.

According to Figure 1, the in-plane engineering strains at the beginning of each time increment (ε_1^{old}, ε_2^{old}, γ_{12}^{old} i.e. $[\varepsilon]_B^{old}$) and the corresponding strain increments ($d\varepsilon_1$, , $d\varepsilon_2$, $d\gamma_{12}$ i.e. $[d\varepsilon]_B$) are calculated internally by Abaqus/Explicit. The next step is to convert the raw material data into the specific form to suit the current constitutive matrix, (i.e. non-orthogonal fibre coordinate system) using coordinate transformations. Material properties are typically given along the fibre directions and defined in a single fibre coordinate system (i.e. an orthogonal system where one base vector is parallel to the fibre direction). For the fabric draping process, the shear deformation can be large, and the two primary yarn orientations may no longer be perpendicular to each other during forming. Although material properties along the fibre direction (such as E_{11}) can be applied in VFABRIC, other properties (such as E_{12}) need to be transformed into the non-orthogonal fibre coordinate system (i.e. the system defined by the warp-fibre vector $\underline{f}_1$, the weft-fibre vector $\underline{f}_2$ and the out-of-plane vector $\underline{f}_3$) using the coordinate transformation matrix Q. Only very minor modifications are required in VFABRIC to establish a non-orthogonal constitutive matrix compared with the more conventional VUMAT approach. Consequently, all the material properties obtained from material testing can be directly used in the non-orthogonal fibre coordinate system. Finally, the stress tensor can be updated from the updated constitutive matrix in the non-orthogonal fibre coordinate system and returned to Abaqus/Explicit for further processing.

2.3. Numerical testing for material model

Simple numerical tests have been performed to verify that the constitutive relations for a biaxial fabric have been implemented correctly in the VFABRIC subroutine. Initial tests were performed on single finite elements, followed by a simulation for a bias extension test. The bias extension geometry is a good verification step, as it induces three distinctly different shear zones due to the boundary conditions. The simulation should return the same force/displacement curve as the input data.

The value for the Young's modulus was taken to be 3.54 GPa in each fibre direction, and the shear modulus was described by the polynomial shown in Figure 2. Results confirm that the constitutive relations implemented via the VFABRIC routine are suitable for defining the in-plane shear deformation for this type of material.

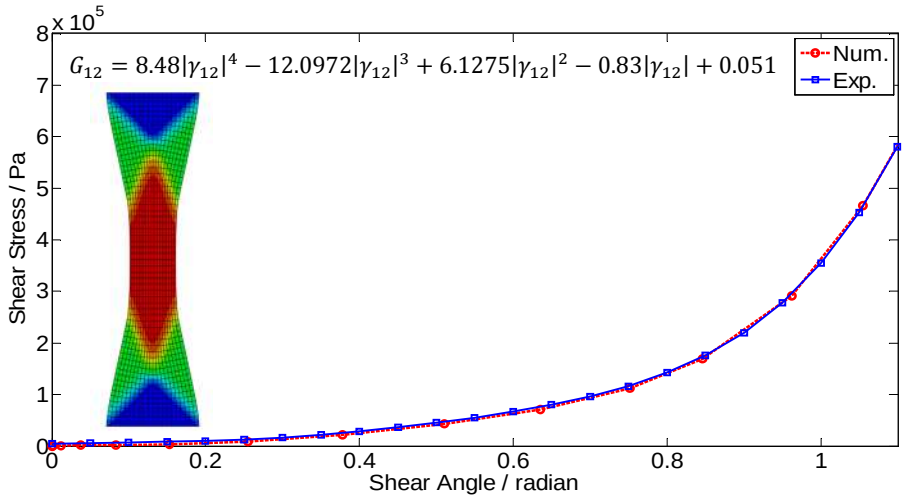

Figure 2. Relationship between shear angle and shear stress from a simulated bias extension test for a balanced plain weave fabric. Experimental data taken from [5].

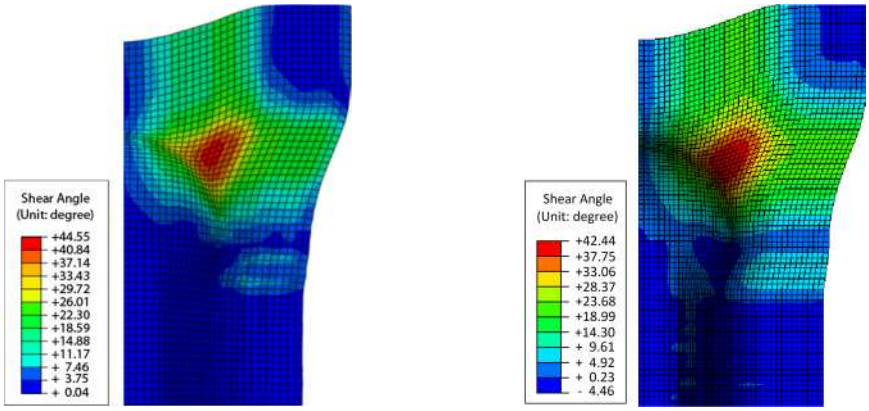

Figure 3. Comparison of Abaqus/Explicit VFABRIC user-defined material model (left) against simulations in the literature [5, 12] (right).

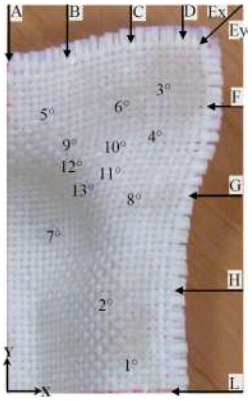

Points	Def. X-Coord. (m)	Def. Y-Coord. (m)	Shear Angle (degree) Num.		Shear Angle (degree) Exp.
			Nott	Lyon	
1	0.088	0.033	0.83	0.26	0.00
2	0.064	0.088	0.78	2.13	1.34
3	0.116	0.219	1.88	4.40	2.80
4	0.091	0.180	9.18	8.84	10.50
5	0.023	0.181	11.22	13.09	15.00
6	0.072	0.192	15.46	16.88	15.50
7	0.038	0.123	16.61	17.80	16.50
8	0.082	0.132	21.86	19.57	22.00
9	0.040	0.157	25.22	26.88	23.45
10	0.060	0.168	30.20	28.34	29.40
11	0.067	0.148	34.67	36.29	33.43
12	0.052	0.136	40.44	42.16	39.00
13	0.045	0.145	37.90	43.18	39.50
Average Error in Magnitude $\frac{1}{N}\sum\lvert\gamma_{12}^{num} - \gamma_{12}^{exp}\rvert$			1.12	1.96	

Figure 4. Comparison of shear angle data from numerical and experimental studies [5, 12] for a 0°/90° plain weave fabric formed using the International Forming Benchmark geometry.

The developed VFABRIC model has been further validated using data from the International Forming Benchmark, available from the Woven Composites Benchmark Forum [14]. There is

a very strong correlation between the results published in [5, 12] and from the VFABRIC model presented here. Figure 3 indicates that shear angle distribution and material draw-in are very closely matched. The local shear angle has been checked at 13 discrete points (coordinates defined in [5]) and compared against numerical and experimental data from [5]. The two peak shear angles differ slightly (5%) between the two models, but according to Figure 4, the VFABRIC approach adopted here produces closer results to the experimental data than the numerical model from [5, 12], with an average error of 1.12° compared to 1.96°.

3. Fabric drape simulation

3.1. Forming simulation for unstitched fabric

Drape simulations were carried out using a hemisphere model with 0.100 m diameter [2] and the same balanced plain weave fabric as in Section 2.3. The model consisted of a matched male punch and female die, with a planar blank holder to apply pressure to the fabric to maintain tension in the tows throughout the forming process. The initial size of each ply was 0.32 m × 0.32 m at a thickness of 0.001 m. The friction coefficient was 0.2 between all fabric plies and between fabric and tool.

Simulations have been performed to study the formability of a single 0°/90° ply and a ±45° ply, as shown in Figure 5. The contour plots show the magnitude of the shear angles at the final stage of the forming process. Clearly, the fibre orientations have a significant effect on the draw-in, as expected. The maximum shear angle for a single 0°/90° layer is 57.92°, which is slightly lower than the value (60.34°) for the ±45° layer. Visual comparisons with data from the literature [15], although obtained for different material properties, suggest that the magnitude of these maximum shear angles are plausible and the degree of draw-in and shear angle distributions are similar.

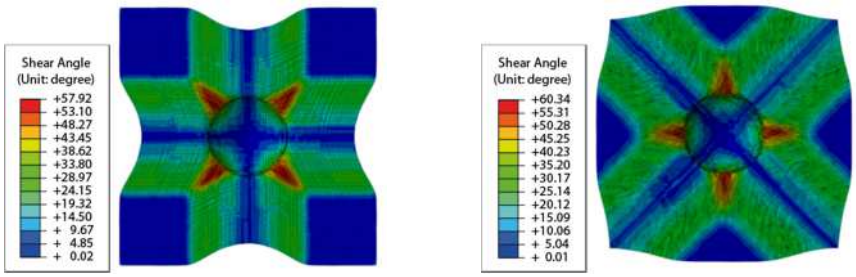

Figure 5. Results of forming simulation (shear angle in degrees); left: single 0°/90° fabric ply (maximum shear angle 57.9°); right single ±45° fabric ply (maximum shear angle 60.34°).

The forming behaviour of two different fabric stacks with the same number of plies in each orientation, but different ply sequences, has been studied. The first lay-up was symmetric $[(0°/90°)/±45°]_s$ and the second asymmetric $[(0°/90°)_2/(±45°)_2]$. The shear angle distributions in the individual plies were found to be very similar to those from the single ply simulations in Figure 5. In Figure 6, the shear angles have been plotted along a diagonal path (centre to corner) for just the 0°/90° plies of both laminates (the ply order was counted from the bottom, i.e. the bottom ply is referred to as 1st ply). This indicates that the ply sequence influences the shear angle distribution, as all four curves in Figure 6 are different between 0.05 m and 0.15 m. It can be concluded that the position of the ply through the thickness (location relative to punch or die) affects the shear angle distribution, but the shear angle is also influenced by the initial orientation of plies in contact. The difference in shear behaviour is expected to become more significant as the laminate thickness increases (number of plies increases).

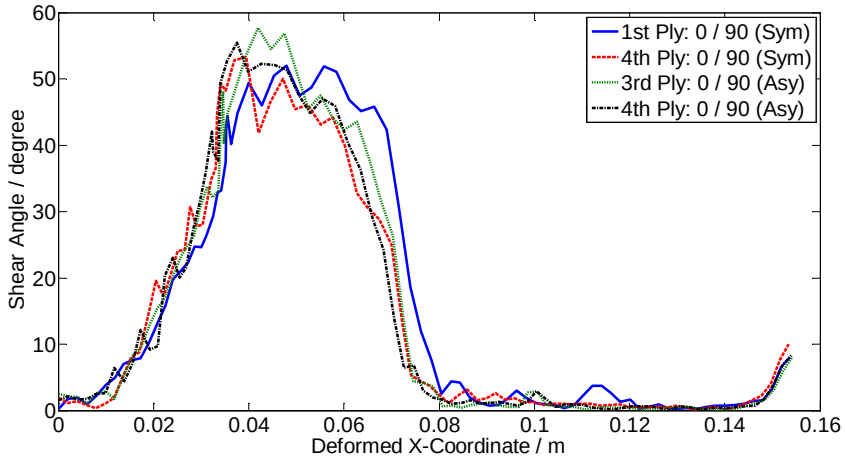

Figure 6. Shear angle along half diagonal (centre to corner) of 0°/90° plies. Plies are taken from two laminate stacks, symmetric $[(0°/90°)/\pm45°]_s$ and asymmetric $[(0°/90°)_2/(\pm45°)_2]$.

3.2. Forming simulation for stitched fabric

In the present work, stitches have been modelled as spring elements in Abaqus/Explicit with a spring constant of 3.76×10^5 N/m. They are used to connect nodes sharing the same in-plane position at the beginning. Their initial length corresponds to the distance between nodes in adjacent plies.

3.2.1 Influence of fabric orientation

Through-thickness stitching around the perimeter of multi-ply preforms with identical ply orientations was found to have no measurable effect on the shear performance, compared with the unstitched case, since the displacement of each ply is almost identical.

Figure 7 shows the forming results for a 4-ply preform with different fabric orientations $[(0°/90°)/\pm45°]_s$, with stitches applied at every node around the perimeter. In this case, stitching clearly influences the forming quality. The most noticeable differences compared to the unstitched lay-up appear in the vicinity of the stitches, where significant local wrinkling occurs. This is related to the relative displacement between unstitched plies, which has a maximum near the mid-point of each edge and minima at the four corners. The maximum shear angles of stacks with and without stitching are quite different, i.e. the former is 56.96° while the latter is 64.68°, although both of them appear in the third ply.

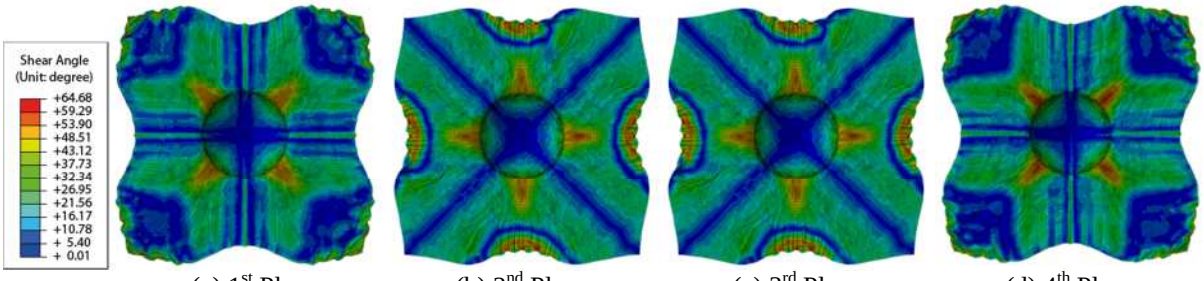

(a) 1st Ply (b) 2nd Ply (c) 3rd Ply (d) 4th Ply

Figure 7. Results of forming simulation for a $[(0°/90°)/\pm45°]_s$ fabric stack with stitching around perimeter (maximum shear angle 64.68° in 3rd ply).

3.2.2 Influence of stitch pattern

Three different stitching patterns have been considered for simulations with $[(0°/90°)/\pm45°]_s$, which include perimeter stitching (Figure 7), cruciform stitching at 0°/90° through the x/y centrelines (Figure 8) and diagonal stitching at ±45° through the four corners (Figure 9).

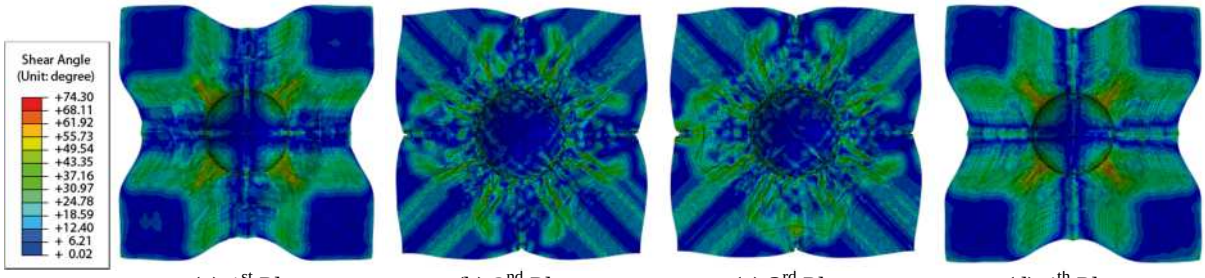

(a) 1st Ply (b) 2nd Ply (c) 3rd Ply (d) 4th Ply

Figure 8. Results of forming simulation for a [(0°/90°)/±45°]s fabric stack with stitching in cruciform (maximum shear angle 74.30° in 1st ply).

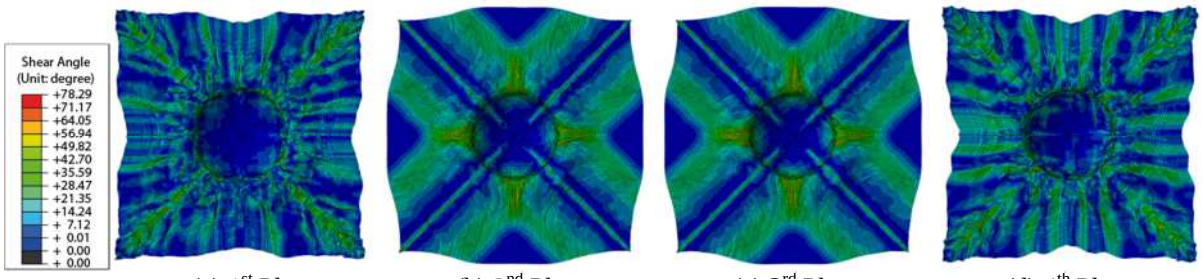

(a) 1st Ply (b) 2nd Ply (c) 3rd Ply (d) 4th Ply

Figure 9. Results of forming simulation for a [(0°/90°)/±45°]s fabric stack with stitching in diagonal (maximum shear angle 78.29° in 4th ply).

Results in Figures 7, 8 and 9 indicate that stitch-bonds influence the global shear angle distribution in each ply of the component rather than having just a localised effect with the most significant effects observed when placing stitches between plies of different orientations. Moreover, the most visible effects on deformation behaviour appears in the plies where the stitching paths go directly through high shear areas, such as the ±45° plies in the cruciform-stitched stack (shown in Figure 8) and the 0°/90° plies in the diagonal-stitched stack (shown in Figure 9). The best quality of the deformed lay-up is achieved by stitching along the perimeter edges (Figure 7), in which case the maximum shear angle (64.68°) is the smallest among all stitching patterns here with fewer wrinkles on the formed hemisphere surface. For the other stitching patterns, unrealistically large maximum shear angles (such as 78.29° in the case of diagonal stitching) occurring in the vicinity of the stitch locations are related to substantial wrinkling on the formed hemisphere surface and indicate issues to be expected in forming of actual fabrics. However, stitching the preform layers along the perimeter may prove difficult in reality. Meanwhile, for the cases where stitching paths go through high shear areas, such as the cruciform in Figure 8 and diagonal in Figure 9 the forming quality is worse than in other cases, although these patterns appear more feasible for automated manufacturing routes.

4. Conclusions

Abaqus/Explicit simulations using the user-defined material model suggest that: (1) the developed material model is suitable for simulating the forming behaviour of multi-ply preforms. CPU times of approximately half an hour on an Intel Core i7 processor with 32GB

of RAM for a model with over 120,000 elements indicate its computational efficiency; (2) the initial fibre orientations of the fabric layers determine drapability and the overall distribution of shear angles; (3) selection of a stitching pattern is a compromise between improving the quality of the preform and the practical feasibility of its implementation. Future work will focus on developing a stitch optimisation algorithm to determine the location and frequency of stitches.

References

[1] Boisse, P., et al., Finite element simulations of textile composite forming including the biaxial fabric behaviour. *Composites Part B: Engineering*, 1997. 28(4): 453-464.
[2] Long, A.C., *Design and manufacture of textile composites*. 2005: CRC press.
[3] Duhovic, M., P. Mitschang, and D. Bhattacharyya, Modelling approach for the prediction of stitch influence during woven fabric draping. *Composites Part A: Applied Science and Manufacturing*, 2011. 42(8): 968-978.
[4] Molnar, P., et al., Influence of drapability by using stitching technology to reduce fabric deformation and shear during thermoforming. *Composites Science and Technology*, 2007. 67(15): 3386-3393.
[5] Khan, M.A., Numerical and Experimental Forming Analyses of Textile Composite Reiforcements Based on a Hypoelastic Behaviour. 2009.
[6] Ten Thije, R. and R. Akkerman, A multi-layer triangular membrane finite element for the forming simulation of laminated composites. *Composites Part A: Applied Science and Manufacturing*, 2009. 40(6): 739-753.
[7] Cheruet, A., et al., Analysis of the Interply Porosities in Thermoplastic Composites Forming Processes. *International Journal of Forming Processes*, 2002. 5(2-3-4): 247-258.
[8] Harrison, P., R. Gomes, and N. Curado-Correia, Press forming a 0/90 cross-ply advanced thermoplastic composite using the double-dome benchmark geometry. *Composites Part A: Applied Science and Manufacturing*, 2013. 54: 56-69.
[9] Bel, S., et al., Finite element model for NCF composite reinforcement preforming: Importance of inter-ply sliding. *Composites Part A: Applied Science and Manufacturing*, 2012. 43(12): 2269-2277.
[10] Sidhu, R., et al., Finite element analysis of textile composite preform stamping. *Composite structures*, 2001. 52(3): 483-497.
[11] Bel, S., et al. Validation of local stitching simulation for stitched NCF ply stacks. In *The 19th International Conference on Composite Materials*, 2013.
[12] Khan, M.A., et al., Numerical and experimental analyses of woven composite reinforcement forming using a hypoelastic behaviour. Application to the double dome benchmark. *Journal of materials processing technology*, 2010. 210(2): 378-388.
[13] Boisse, P., Finite element analysis of composite forming, in *Composite Forming Technologies*, A. Long, Editor. 2007.
[14] Cao, J. Woven Composites Benchmark Forum, *http://www.wovencomposites.org*. Accessed September 2013.
[15] Boisse, P., et al., Simulation of wrinkling during textile composite reinforcement forming. Influence of tensile, in-plane shear and bending stiffnesses. *Composites Science and Technology*, 2011. 71(5): 683-692.